PREDICTION OF TWO-PHASE RELATIVE PERMEABILITY IN POROUS MEDIA BASED ON NETWORK MODELING OF LATTICE GAS AUTOMATA

by

Dedy Kristanto and Mariyamni Awang

I. INTRODUCTION

The displacement of one fluid by another is controlled by the geometry of the pore space. The relative hydrodynamic conductance of each fluid at a given saturation is the relative permeability, while the pressure difference between the phases is the capillary pressure. These two functions determine the macroscopic fluid flow behavior in hydrocarbon reservoir over the scale of centimeters to kilometers.

At the pore scale fluids reside in intergranular space of typical sedimentary rocks. The rock type and fluid properties are likely to change drastically through the reservoir, the only sample of rock come from drilling wells, which represents a tiny fraction of the total volume in a reservoir. Furthermore, relative permeability measurements on these samples are difficult and time consuming. To quantify and control uncertainty in recovery estimations, it is necessary to have some theoretical understanding of transport properties. Such understanding would enable us to predict the sensitivity of relative permeability to geological factors such as porosity, and the nature of the fluids. This work is a preliminary step in this direction. A more important result from this work is that we are now able to quantify the change in the relative permeability to those geological factors.

In this paper a pore structure and displacements mechanisms to model two-phase flow in porous media were constructed using lattice gas automata. The void space of the media is represented as a network of large spaces (pores) connected by narrower throats. The aggregation of cell pore volumes is used to calculate the porosity of the network and the fluid saturation when different cells are occupied by different fluids. By judicious choices for the distribution of pore and throat sizes of the network it is possible to predict relative permeability. For predicting the absolute and relative permeability, it is assumed that the viscous pressure drops occur across the throats.

II. LATTICE GAS AUTOMATA

Lattice gas models belong to the class of cellular automata and consist of a set of lattices, where the intersection points of the lattices take a finite number of states. The automaton evolves in discrete time steps. The state of each site at any time is determined by its own state and the state of a set of neighboring sites at the previous time step. A lattice gas model in which the state of the fluid needs to be known only at the lattice sites and only at discrete times can run fast on a computer. The lattice gas model has another advantage since all the collisions occur at the same time. This is a particular advantage if the simulation is being run on a parallel computer. These two times saving advantages of a lattice gas model allow simulations of a significantly large scale to be performed.

The evolution of the system on time-step to the next takes place in two successive stages, i.e., streaming (propagation) stage and collision stage. At the start of each time step the particles at each site collide according to the particular collision rules for the model being used - the collision stage. After the collision stages each particle travels in a straight line along one of the lattice links, unless it is a rest particle, until it arrives at the next link - the streaming stage. The particles arriving at their new sites then collide at the beginning of the next time step.

The collision phase of each time step is the process of transformation between the input and output states of the lattice sites under a set of collision rules. The collision rules are Boolean expression, which define the relationship between the input and output states of a site and which satisfy the following minimum requirements that collision rules should: conserve mass and momentum, avoid spurious conserved quantities (invariants), in-

variant under all transformations that preserves the velocity set, conserve probability, and satisfy semi-detailed balance.

In the FHP models of lattice gas automata, each link of the hexagonal lattice may carry one particle (of the given mass/momentum/energy state) at any one time. This is called exclusion principles. The particles of fluid live on a hexagonal lattice, as shown in Figure 1. Figure 1 shows that each arrow represents a particle of unit mass moving in the direction given by the arrow. The lattice is initially prepared so that no more than one particle is moving with a particular velocity at a particular site on the lattice (Figure 1a). Then, the particles hop and scatter, as illustrated by Figure 1b; each particle moves one lattice unit in the direction of its velocity. Scattering is shown in Figure 1c; if two or more particles arrive at the same site, they can collide. Some collisions cause the particle to scatter their velocity change. In all cases, however, collisions may change neither the total number of particles nor the vector sum of the velocities. The only collisions that have changed the configuration of particles are located in the middle row. In other words, mass and momentum are conserved.

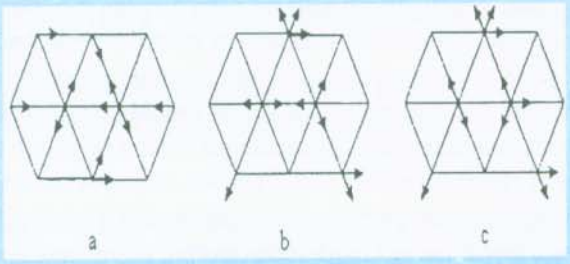

Figure 1
One time step in the evolution of the FHP models, (a) is the initial condition, (b) the propagation step of the particles, and (c) the result of collisions step of the particles

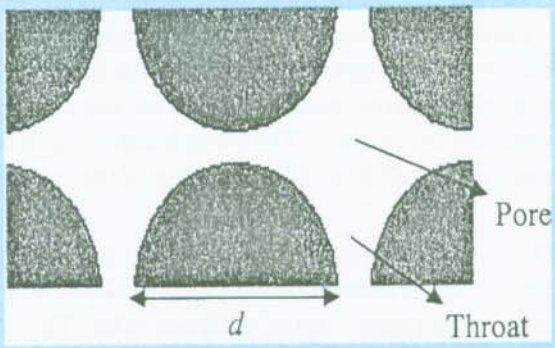

Figure 2
Schematic of porous media studied, where the porous media is considered to be an array of pore connected by narrow throats

The particle dynamics depicted in Figure 1 are expressed by the equation,

$$n_i(x + c_i, t + 1) = n_i(x, t) + \Delta_i[n(x, t)] \qquad (1)$$

Here the time t is integer-valued and the duration of a time step is taken to be unity. The quantities $n = (n_1, n_2, \ldots, n_6)$ are Boolean variables that indicate the presence (n_i=1) or absence (n_i=0) or particles moving from a lattice site situated at position x to the neighboring site situated at position $x + c_i$, where the particles move with unit speed in the directions given by equation,

$$c_i = \left(\cos\frac{\pi i}{3}, \sin\frac{\pi i}{3}\right), \quad i = 1,2,\ldots,6. \qquad (2)$$

The function D_i is called the collision operator. It describes the change in $n_i(x,t)$ due to collisions, and takes on the values 0, 1 and –1.

III. SIMULATION MODEL

This paper presents a pore-network model of two immiscible fluids using lattice gas automata based on a pores-and-throats representation of the porous media. The simulation conducted on the 800x600 lattice sizes. In this network model, the pores are arranged on the hexagonal lattice (FHP-II model) of lattice gas automata and each pore is connected to up six throats, where the pores connecting two adjacent nodes may have a uniform diameter, or it may consist of pores segments with different diameters that represent porous media.

In order to make progress in the study of immiscible fluid displacement in porous media, it is therefore necessary to simplify either the rock geometry or the fluid flow. In two dimensions, it could construct a simplified model of a single pore, and porous media modeled as a network of such interconnected pores. The fluid flow of two-phase fluid through such a network is modeled based on the assumption about the flow in these interconnected pores. The simplified model of granular pore space as an array of wide pore interconnected by narrower regions, which is called throats is illustrated in Figure 2.

VOL. 27. NO. 1 MARET 2004: 3 - 10

Furthermore, in order to determine the macroscopic properties of heterogeneous porous media, the absolute porosity of the porous media is determined by,

$$\phi = \left(1 - \frac{V_0}{V}\right) \tag{3}$$

where V_0 is the volume of the obstacles, and V is volume in two-dimensional space, while the value of effective porosity is given by equation

$$\phi_{eff} = ax^3 - (2a + \phi_C)x^2 + (a + 1 - \phi_C)x \tag{4}$$

where

$$x = \frac{(\phi - \phi_C)}{(1 - \phi_C)} \tag{5}$$

and a is constant ($a = 0.3$), and ϕ_C is a critical porosity or percolation threshold, respectively. The permeability coefficient (k) of porous media is determined by Carman-Kozeny equation,

$$k = \frac{\phi_{eff}^{\ 3}}{c\tau^2 S^2} \tag{6}$$

where c is the Kozeny coefficient, f_{eff} is the effective porosity of the porous media, τ is the tortuosity of the porous media, and S is the specific surface area, respectively.

When carbon dioxide occupies the center of the pore or throat, oil will remain in throat of the pore space, which is to be the fraction of the cross-section occupied multiplied by the total pore volume. Thus the carbon dioxide phase volume is the total (bulk) volume of an element minus the volume of the oil phase. Saturations for each phase (oil and gas) are found by adding the volumes of each phase in all pores and throats and dividing by the total pore volume of the model. It gives both oil and gas saturations, which could be calculated from the following equations,

$$S_o = \frac{V_o}{V_p} \tag{7}$$

and

$$S_g = 1 - S_o \tag{8}$$

where V_o is oil volume and V_p is the pore volume of a porous media. The pore volume is calculated by,

$$V_p = V_b\, \phi_{eff} \tag{9}$$

where ϕ_{eff} is an effective porosity as given by Equation (4).

In this model, the relative permeability of oil and gas phases in porous media is calculated using Corey's formulas as follows,

$$k_{ro} = \left(\frac{S_o}{1 - S_{or}}\right)^4 \tag{10}$$

and

$$k_{rg} = \left\{1 - \left(\frac{S_o}{1 - S_{or}}\right)^2\right\}\left\{1 - \frac{S_o}{1 - S_{or}}\right\}^2 \tag{11}$$

where k_{ro} is the relative permeability of oil, k_{rg} is the relative permeability of gas, S_o is oil saturation, and S_{or} is the residual oil saturation, respectively.

IV. RESULTS AND DISCUSSION

In order to predict the macroscopic properties of porous media, it is crucial to know the threshold porosity for filling, and the permeability of each pore and throat. The pore and throat used to define threshold porosity (ϕ), where in this simulation the threshold porosity (ϕ_c) used is 5%. The effective porosity (ϕ_{eff}) was estimated by using Equation (4), while the permeability (k) was estimated by Carman-Kozeny equation (Equation 6). Furthermore, the pore volume (PV) is calculated by Equation (9), where in porous media is completely filled with oil. Summary of the simulation results is shown in Table 1.

Table 1
Summary of the simulation results

ϕ (%)	ϕ eff (%)	k (mD)	PV
9.778	6.126	4.441431	2.940594
14.837	12.278	16.86075	5.893439
19.822	18.034	38.83125	8.656466
24.81	23.511	74.78043	11.28547
29.922	28.861	130.3054	13.85328
34.844	33.784	213.4396	1621632

Figure 3 shows the simulated effective porosity as a function of absolute porosity of porous media. It is obvious from this plot that the effective porosity curves tend to be linear, and had a value below the absolute porosity of porous media constructed. The effective porosity value was 6.126% to 33.784%.

As mentioned previously, the permeability was predicted using Carman-Kozeny equation (6), where the trend of permeability with effective porosity resulted from this simulation shows a good prediction as presented in Figure 4. This demonstrates that the model and its network representation of the pore space was adequate to predict the properties and behavior of fluid flow in porous media, which implies that the major flow paths have been accurately identified. The permeability of heterogeneous porous media had ranges of 4.44143 mD to 213.4396 mD.

Figure 5 presents the pore volume change as a func-

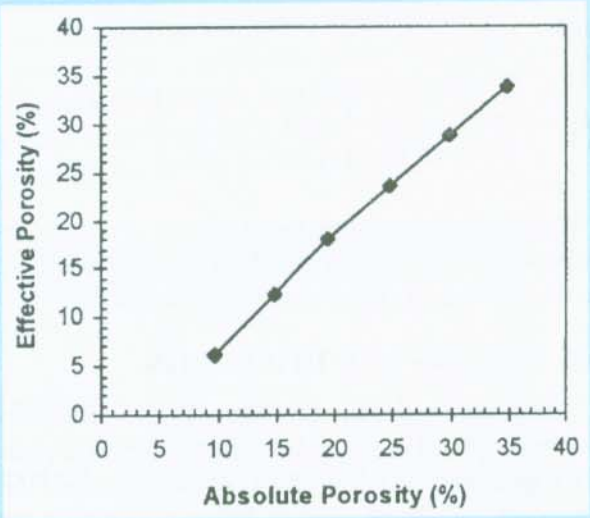

Figure 3
Simulated effective porosityas a function of absolute porosity

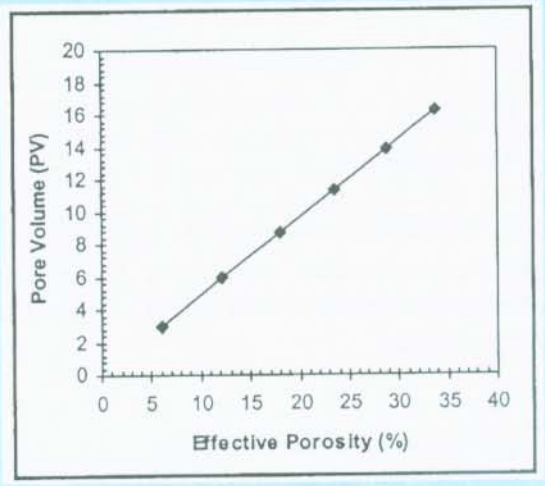

Figure 5
Pore volume of porous mediaas a function of effective porosity

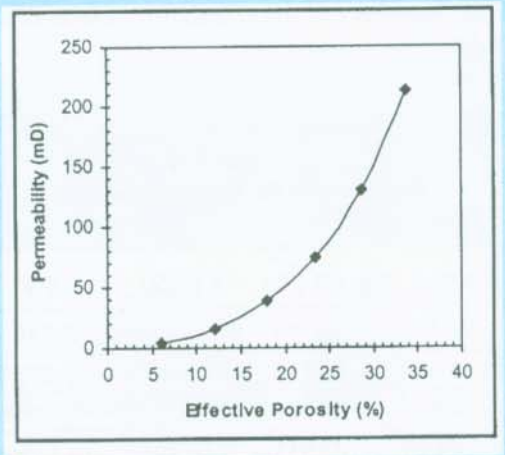

Figure 4
Permeability of porous mediaas a function of effective porosity

Table 2
Residual oil saturation results from oil and gas relative permeability curves

Effective poroosity (%)	Residual Oil saturation (%)
6.126	16.4883
12.278	8.7266
18.034	6.1833
23.511	5.1268
28.861	4.3041
33.784	3.8211

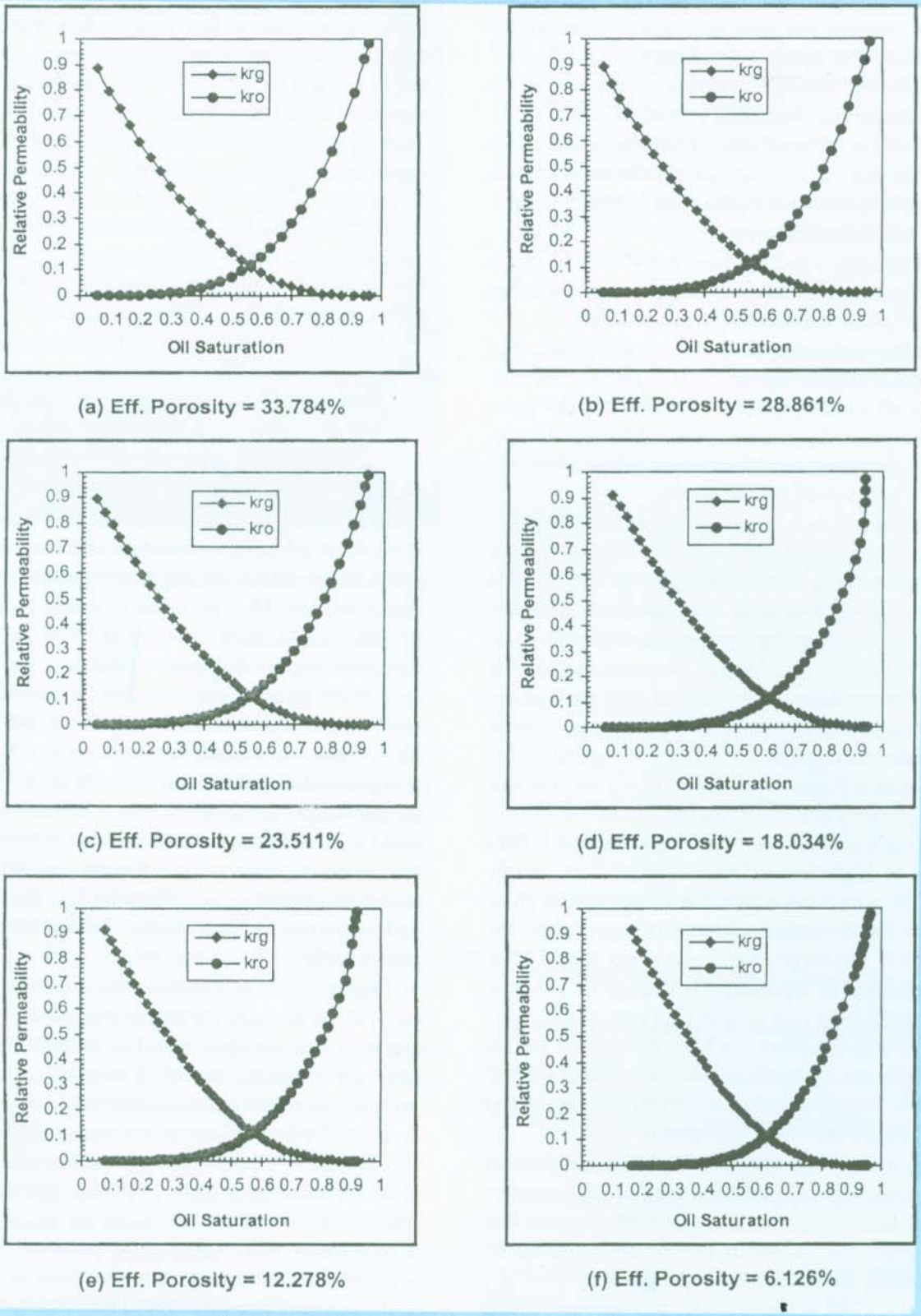

Figure 6
Relative permeability curves for effective porosity of porcus media ranges of 33.784% to 6.126%

tion of effective porosity of porous media. It shows that with the increasing in effective porosity of porous media, the pore volume that could be occupied by the fluids also increases. The trend of these curves was also linear. Based on the effective porosity of porous media, the pore volume had ranges of 2.940594 to 16.21632 lattice units^3. The value of pore volume is an important parameter in order to estimate the distribution of fluids in porous media, which is represented by the fluid saturations of oil (So) and gas (Sg).

Based on data listed in Table 1 and also Figure 3 through Figure 5, it is obvious that the model used to simulate two-phase immiscible fluids displacement is well established to predict the rock properties of porous media. The flow configuration and the fluids distribution were very much affected by the microstructure of the pore-grain of porous media, which can be modeled precisely. This means that these model parameters reproduce representative behavior of porous media.

Furthermore, in two-phase immiscible fluids displacement, the gas is injected into porous media that is originally occupied by oil, so that the two fluids will reside in the pore space. At low flow rates the fluid motion is controlled by capillary forces and move through these pore spaces with no interaction between the phases, where the permeability is associated with each phase. This fraction is then represented by relative permeability, which depends purely on the fluid configuration at a given saturation. Relative permeability is a macroscopic transport property that describes the simultaneous flow of immiscible fluids displacement in porous media. For a given type of displacement process, relative permeability might be written as a function of one of the phase saturations. In this work, the relative permeability of gas (k_{rg}) and oil (k_{ro}) were predicted using the Corey's equation as described in Equations (10) and (11). The relative permeability curves of gas (k_{rg}) and oil (k_{ro}) as a function of gas saturation (S_g) were obtained for the ranges of effective porosity of porous media of 6.126% to 33.784%. The simulated results of oil and gas relative permeability are presented in Figure 6.

Figure 6 shows the simulated relative permeability of oil (k_{ro}) and gas (k_{rg}) as a function of oil saturation (S_o). From the simulation results presented in this Figure, it is clear that for porous media that has lower effective porosity value, the relative permeability of oil (k_{ro}) will also lower. An explanation for this behavior can be written as that for porous media structure with large pores and correspondingly small surface areas, the end points of the oil relative permeability curves are high and large saturation change may occur during the two-phase flow. By contrast, the porous media structure with small pores have larger surface areas, where under this conditions the end point of the oil relative permeability curves are lower and the saturation change during two-phase flow is smaller. It is obvious from these Figures that pore geometry could have the most profound effect on the relative permeability. Furthermore, qualitatively the relative permeability curves had similar trends for each value of effective porosity. The difference is trapping that affected the residual oil saturation obtained. It is shown that the porous media have correlations in both pore size and connectivity.

From Figure 6, also it could be shown that from each oil and gas relative permeability curves (k_{ro} and k_{rg}) as a function of oil saturation (S_o), there are three important characteristic points to observed, are: (a) the oil relative permeability (k_{ro}) declines rapidly for a small increases in gas saturations (S_g); (b) it indicates an equilibrium gas (S_{gc}), the saturation at which gas begins to flow; (c) it indicates the residual oil saturation (S_{or}), the value below which the oil saturation could not be reduced by gas. In Figure 6a, at effective porosity of 33.784% for example, starting at 100% gas saturation, the curves show a decrease in oil saturation to 0.038211 (a 0.96289 increase gas saturation) and reduction in the relative permeability to gas (k_{rg}) from 100% down to 88%, where at 0.038211 oil saturation (S_o), the relative permeability to oil is essentially zero. The value of oil saturation 0.038211 in this case, is residual oil saturation (S_{or}). Similarly, the loss of relative permeability to gas phase (k_{rg}) exists when the gas saturation reduced to the gas saturation equilibrium (S_{gc}). The residual oil saturation results from relative permeability curves is shown in Table 2.

From Figure 6, it is also shown that decreasing the porosity could shifts the relative permeability curves to the right side and hence higher residual oil saturation obtained. The cross lines of oil relative permeability (k_{ro}) with the gas relative permeability (k_{rg}) curves are higher than 0.5 (50%) of oil saturation value, which means that the system is oil wet. The reason for this is that the fluids invaded large paths of porous media network in sequence of pore size, leading to a channeled displacement when these paths connect. The result is increase in oil trapping and an increase in gas relative permeability at low saturation. This result is relevant with the result of Yortsos *et al.* (1993), that the oil (wetting phase) could be macroscopically trapped in low permeability regions.

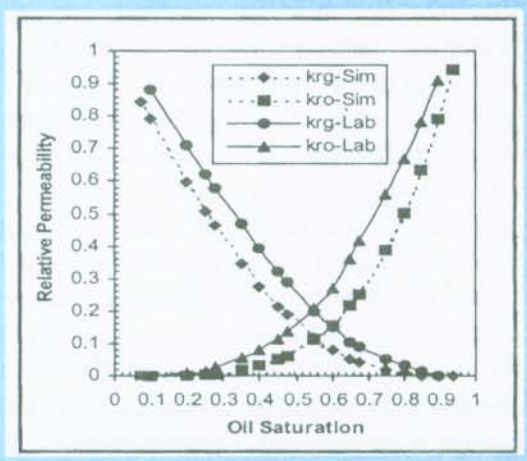

Figure 7
Comparison of relative permeability curvesas a function of oil saturation fromsimulation and laboratory experiment

Figure 7 shows the comparison of the simulated relative permeability with the result from laboratory experiment. The comparison conducted on the effective porosity of both relative permeability results were quite close, each being 23.511% for simulated relative permeability and 22.7% for laboratory experiment. While, the permeability of simulation have 74.78043 mD, and 148.65 mD for laboratory experiment, respectively. From Figure 7, it is shown that the simulated relative permeability had similar trend with the laboratory experiment. The dash lines were the relative permeability of oil (k_{ro}) and gas (k_{rg}) predicted by the simulation, while the full lines were the relative permeability of oil (k_{ro}) and gas (k_{rg}) measured from the laboratory experiment, respectively. The cross lines of simulated relative permeability is achieved at the gas saturation of 0.56, and for the laboratory experiment at the gas saturation 0.55, it means that both had the same condition, i.e. oil wet system. From the relative permeability value view point, the cross lines of simulated relative permeability is lowest compared with the laboratory experiment, were 0.12 for simulation and 0.21 for laboratory experiment. The reason of these phenomena is due to the simulation and laboratory experiment had the different permeability. The cross lines in the system means that the permeability to both oil and gas is the same and each fluid can move with equal freedom through the porous media under these conditions. Based on the Figure 7, it is shown that the simulation model is an adequate representation of the geometry of pore space as in laboratory experimental.

V. CONCLUSIONS

1. Relative permeability is a macroscopic transport property that describes the simultaneous flow of immiscible fluids in porous media.
2. Porous media have correlations in both pore size and connectivity.
3. Decreases on the effective porosity of porous media could shifts the relative permeability curves to the right side.
4. Pore geometry could have the most profound effect on the relative permeability.
5. The relative permeability for every phase shows a functional dependence upon the saturations of two-phase as well as fluid properties.
6. The simulation results obtained have a reasonable good agreement with the laboratory experiment.

NOMENCLATURE

a = constant ($a = 0.3$)
c = the Kozeny coefficient
k = permeability of porous media, mD
k_{ro} = relative permeability of oil
k_{rg} = relative permeability of gas
S_o = oil saturation, fraction
S_g = gas saturation, fraction
S_{or} = residual oil saturation, fraction
S = the specific surface area
V_0 = volume of the obstacles
V = volume in two-dimensional space
V_o = oil volume in porous media
V_p = the pore volume of a porous media
ϕ = porosity of porous media, fraction
ϕ_{eff} = effective porosity of porous media
ϕ_C = critical porosity or percolation threshold
τ = the tortuosity of the porous media

ACKNOWLEDGEMENTS

The authors thank the Petroleum Engineering Department of University of Technology Malaysia, for the support and permission to publish this paper. DK also would like to thank the Universitas Pembangunan Nasional "Veteran" Yogyakarta for giving permission and opportunity to conduct the research at the University of Technology Malaysia. In addition this research is funded by the Government of Malaysia under the Intensification of Research Priority Areas (IRPA) program Vote No: 72027.

REFERENCES

1. Blunt, M. J., King, M. J., and Scher, H., 1992 : "Simulation and Theory of Two-phase Flow in Porous Media", Physical Review A, 46, p.7680 - 7699.
2. Blunt, M. J., and Scher, H., 1995 : "Pore-level Modeling of Wetting", Physical Review A, 46, p.7680 - 7699.
3. Blunt, M. J., 1997 : "Physically Based Network Modeling of Multiphase Flow in Intermediate-Wet Porous Media", Journal of Petroleum Science and Engineering, 14, p.1 - 14.
4. Boghosian, B. M., and Coveney, P. V., 2000 : "A Particulate Basis for an Immiscible Lattice-Gas Model", Computer Physics Communications, 129, p.46 - 55.
5. Collins, R. E., 1976 : *Flow of Fluids through Porous Material*, PennWell Books, Tulsa-Oklahoma.: PennWell Publishing Co., p.3 - 26; and 139 - 149.
6. Dullien, F. A. L., 1992 : *Porous Media: Fluids Transport and Pore Structure*, New York.: Academic Press, Inc.
7. Frisch, U., Hasslacher, B., and Pomeau, Y., 1986 : "Lattice-Gas Automata for the Navier-Stokes Equation" , *Physical Review Letters,* 56, p.1505 - 1508.
8. Frisch, U., d' Humières, D., Hasslacher, B., Lallemand, P., and Pomeau, Y., 1987 : "Lattice Gas Hydrodynamics in Two and Three Dimensions", *Complex Systems,* 1, p.649 - 707.
9. Kadanoff, L. P., McNamara, G. R., and Zanetti, G., 1989 : "From Automata to Fluid Flow: Comparison of Simulation and Theory", Physical Review A, 40, p.4527 - 4541.
10. Kharabaf, H., and Yortsos, Y. C., 1996 : "A Pore-Network Model for Foam Formation and Propagation in Porous Media", SPE Annual Technical Conference and Exhibition. Denver, p.779 - 790.
11. Koponen, A., Kataja, M., and Timonen, J., 1997 : "Permeability and Porosity of Porous Media", Physical Review E, 56, p.3319 - 3325.
12. Kristanto, D, and Awang, M., 2001 : "Determination of the Permeability and Porosity of Porous Media by Lattice Gas Automata Method", MSTC01-B-82, Malaysian Science and Technology Congress (MSTC) 2001, Melaka, Malaysia, 8-10 October.
13. Kristanto, D, and Awang, M., 2002 : "Simulation of Two-phase Reservoir Fluids Separation by Immiscible Lattice Gas Automata", 4ASTC-A-13, 4th Asian Science and Technology Congress (4ASTC) 2002, Kuala Lumpur, Malaysia, 25-27 April.
14. Kristanto, D, and Awang, M., 2003 : "Lattice Gas Automata Simulations to Determine the Macroscopic Properties of a Porous Medium", Advanced Technology Congress (ATC) 2003 in the Conference on Advances Theoretical Sciences (CATS), Putrajaya - Kuala Lumpur, Malaysia, 20-21 May.
15. Kristanto, D, and Awang, M., 2003 : "Estimation of Surface Tension for Two Immiscible Fluids Using Lattice Gas Automata", SPE 84892, Society of Petroleum Engineers International on Improved Oil Recovery Conference in Asia Pacific (SPE-IIORC), Kuala Lumpur, Malaysia, 20-21 October.
16. Larson, R.G., Davis, H. T., and Scriven, L. E., 1981 : "Displacement of Residual Nonwetting Fluid from Porous Media", Chemical Engineering Science, 36, p.75 - 85.
17. Oren, P. E., and Pinczewski, W. V., 1995 : "Fluid Distribution and Pore-Scale Displacement Mechanisms in Drainage Dominated Three-phase Flow", Transport in Porous Media, 20, p.105 - 133.
18. Rege, S. D., and Fogler, H. S., 1987 : "Network Modeling for Straining Dominated Particle Entrapment in Porous Media", Chemical Engineering Science, 42, p.1553-1564.
19. Rothman, D. H., 1988 : "Cellular-automaton Fluids: A Model for Flow in Porous Media", Geophysics, 53, p.509 - 518.
20. Rothman, D. H., and Keller, J. M., 1988 : "Immiscible Cellular-Automaton Fluids", *Journal of Statistical Physics*, 52, p.1119 - 1127.
21. Rothman, D. H., and Zaleski, S., 1997 : *Lattice Gas Cellular Automata: Simple Models of Complex Hydrodynamics*, London, UK.: Cambridge University Press, p.12 - 60; 151 - 165; and 203 - 232.
22. Sheng, P., and Zhou, M. Y., 1988 : "Dynamic Permeability in Porous Media", Physical Review Letters, 61, p.1591 - 1594.
23. Sandrea, R., and Nielsen, R., 1994 : *Dynamics of Petroleum Reservoirs Under Gas Injection*, Houston, Texas.: Gulf Publishing Company, p.58 - 92.
24. Wolfram, S., 1986 : "Cellular Automaton Fluids 1: Basic Theory", *Journal of Statistical Physics,* 45, p.471 - 529.
25. Zaleski, S., and Appert, C., 1990 : "Lattice Gas with a Liquid-Gas Transition", *Physical Review Letters*, 64, p.1 - 4. •